osteophytes. The subchondral sclerotic-cyst serration is accompanied by interposed soft-tissue articulation on the T1 MRI versus CT imaging. T1ρ quantification describes areas of normal PG-rich cartilage, with widespread heterogeneity likely arising from the thinness and abnormal composition of the remaining tissue.

Conclusions: Ankle distraction surgery offers an effective alternative treatment for end stage OA, which allows young patients to preserve their native joints throughout the most productive years of their lives. By delaying the need for joint sacrificing surgeries for over a decade, ankle distraction not only minimizes complications of joint sacrificing surgeries such as adjacent joint arthritis following ankle arthrodesis but also increases implant longevity to later revision TAA.

478
COMPREHENSIVE MORPHOLOGICAL CHARACTERISATION OF OSTEOARTHRITIS IN A PRECLINICAL RABBIT TRAUMA MODEL USING MICRO COMPUTED TOMOGRAPHY

K.S. Stok †, K. Atal †, T.H. Steiner †, A. V. Villarreal Escudero †, M. Wilke ‡, A. Quintin ‡, M.A. Zulliger §, R. Müller †, D. Nesic ‡. † *ETH Zurich, Zurich, Switzerland;* ‡ *Univ. of Bern, Bern, Switzerland;* § *Scanco Medial AG, Brüttisellen, Switzerland*

Purpose: Osteoarthritis (OA) is a slow-developing, chronic disease, with concomitant structural changes in bone and cartilage. Current efforts in clinical research aim to identify disease-modifying osteoarthritis drugs (DMOADs) that would prevent or reverse structural deterioration underlying pathophysiological progression. Preclinical research can assist this effort by investigating therapeutic targets for cartilage regeneration, biomarkers for understanding joint breakdown, and reconstructive approaches for restoring joint health, via novel animal models and innovative technologies. Previously we demonstrated the methods to clearly define cartilage boundaries in a rat OA trauma model, as well as new metrics for sensitive discrimination of structural deterioration. The aim of this work is to demonstrate the scalability of the protocol using a preclinically relevant larger animal model, i.e the rabbit. Comparatively, the cross-section of the rabbit knee is four times larger than the rat.

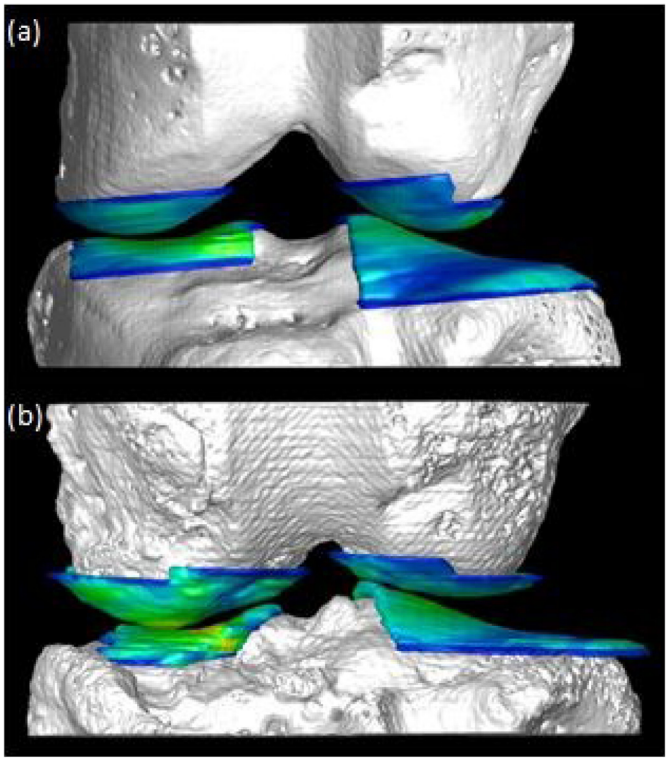

Fig. 1. Three-dimensional reconstruction of the rabbit (a) contralateral, NO and (b) operated, OP knee joint. Lateral aspects are to the left, and medial to the right (where OP has been mirrored to ease comparison). Colour indicates cartilage thickness, where blue is thinnest and yellow towards red is thickest.

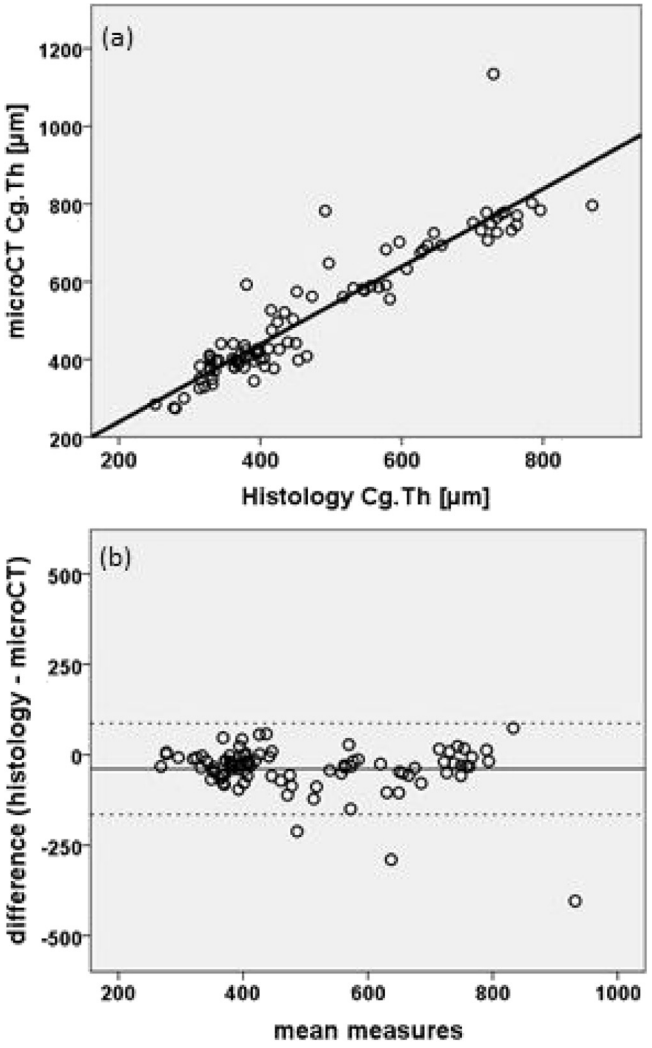

Fig. 2. (a) Plot of 2D cartilage thickness measured by microCT against histology, $R = 0.94$, $p < 0.001$, and (b) a Bland-Altman plot showing the spread of scatter points is relatively even at both low and high values of the mean measures, and thus there is no obvious trend of increasing scatter with Cg.Th.

Methods: Eight 4.5-month old New Zealand white rabbits underwent anterior cruciate ligament (ACL) desmotomy on one knee (OP), where the non-operated contralateral joint served as a control (NO). Animals were sacrificed 8 weeks post-op, the joint space filled with a contrast agent, and scanned using micro-computed tomography, microCT (SCANCO Medical AG; 18 µm voxel size). Scans were rotated to a common orientation from which whole joint changes could be calculated. The cartilage was manually segmented, figure 1. After scanning, joints were dissected and prepared for histology staining with Safranin O-Fast Green. Three histology slices were taken from each femur and tibia ($n = 48$), and registration with microCT allowed identification of the corresponding microCT slice. 2D cartilage thickness (Cg.Th) from both images was correlated. 3D Cg.Th, joint space width (JSW), contact area between femur and tibia when loaded virtually, and the distance (λ) and orientation (α, β, γ) of the centre of mass of the femur relative to that of the tibia along the three principle axes were measured. A univariate analysis of variance was used to test significant differences, $p < 0.05$.

Results: The correlation between 2D Cg.Th from histology and microCT is shown in figure 2a. Correlations were similar for OP and NO, so the data were pooled ($R = 0.94$, $p < 0.001$). Thickness measured by histology was approximately 10% less than microCT. A Bland Altman plot (Fig. 2b) reveals no trend to increased spread with increasing Cg.Th. In 3D, Cg.Th was significantly different in the lateral condyle between NO and OP, where OP cartilage was thicker (NO: 426 ± 53 µm, OP: 495 ± 43

μm). JSW was also significantly larger in the lateral joint in OP (1.94 ± 0.56 mm) than NO (1.37 ± 0.27 mm). When the femur was virtually loaded onto the tibia, two results were apparent; firstly, the distance to first contact mimicked the results of JSW, and secondly, once contact was reached, the contact area with additional steps increased evenly in the lateral compartment for both NO and OP, but increased dramatically in the medial OP compartment. This indicates an altered surface conformity in the medial compartment, a result which is not available from any other metric. Finally, the centre of mass of the femur relative to that of the tibia along the three principle axes indicated an increased destabilisation in the OP joints, where α and γ showed significantly increased variance; (α, γ) for NO (4.6°, 1.9°) and OP (8.9°, 5.3°).

Conclusions: The results of this study show that ACL desmotomy in a rabbit knee joint leads to an increase in Cg.Th and JSW in the lateral condyle. It is possibly due to altered joint biomechanics leading to unloading on this compartment, allowing the cartilage to swell and increasing JSW. Despite this, there is no significant change to contact area, indicating that joint conformity is unchanged. In contrast, medially, a significantly altered contact is seen. This may be due to either a change in conformity, or is related to the instability of the femur and tibia as indicated by the variance in α and γ. The preclinical imaging protocol first introduced in smaller rat joints, has been successfully upscaled to rabbits, as indicated by both the comparison to histology, and the ability to derive sensitive metrics from the data. Ongoing work involves calculating bone morphometry to correlate spatially relevant structural change with joint mechanics and cartilage tissues.

479
OSTEOARTHRITIS PAIN PREDICTION USING X-RAY FEATURES: DATA FROM OAI

J.I. Galvan-Tejada †, V. Treviño †, S. Totterman ‡, J.G. Tamez-Pena †. † *ITESM, Monterrey, Nuevo Leon, MEXICO;* ‡ *Qmetrics Technologies, Rochester, NY, USA*

Purpose: Knee pain is a common and disabling symptom in Osteoarthritis (OA). Joint pain is a late manifestation of osteoarthritis, in earlier stages of the disease; changes in joint structures osteophytes, cartilage degradation, and joint space reduction are shown. Since in developing countries the access to MRI is very limited the main objective was to determine what early radiological evidence is associated with future development of joint pain symptoms.
Methods: OAI datasets used in this work were: "Central Assessment of Longitudinal Knee X-rays for Quantitative JSW" Ver. 1.6, (Quantitative data), and the "Central Reading of Knee X-rays for K-L Grade and Individual Radiographic Features of Knee" Ver. 1.6 (Semi-quantitative data). The 60 months, "Right knee symptom status" as a predictive variable. Subjects were selected from the dataset using some criteria; a) Control subjects should not present pain as a symptom, no symptomatic status, and take no pain medication between baseline date and the 60 month visit, b) Case subjects, in the baseline information shouldn't present pain, no symptomatic status, and no medication, during the study but they should present pain as a symptom in some time point. For quantitative analysis 163 subjects were selected: a) 65 case subjects (27:38 Males:Females), height mean 1688.64 mm, height S.D. 88.03 mm, BMI mean 27.05, BMI S.D. 4.33, Age mean 62.69, age S.D. 9.58, max age 78, min age 46, b) 98 control subjects (43:55 Males:Females), height mean 1680.39 mm, height S.D. 97.91 mm, BMI mean 26.27, BMI S.D. 3.99, age mean 61.80, age S.D. 10.09, max age 79, min age 45. For semi-quantitative analysis 123 subjects were selected: a) 63 case subjects (28:35 Males:Females), height mean 1657.75 mm, height S.D 227.73 mm, BMI mean 27.27, BMI S.D. 4.38, age mean 65.02, age S.D. 9.58, max age 78, min age 46, b) 60 control subjects (34:26 Males:Females), mean height 1691.48 mm, height S.D. 103.28 mm, BMI mean 28.48, BMI S.D. 4.09, age mean 66.72, age S.D. 8.71, max age 79, min age 47. For quantitative data, a height and gender adjustment was performed using a linear regression in order to eliminate a gender size bias, 18 individual right knee features were used in the multivariate analysis. For semi-quantitative data 19 right knee individual features were used in the multivariate analysis. Three multivariate analyses were performed on each semi-quantitative and quantitative data. T0, using the information about the first appearance of pain as a symptom, data were analyzed using the 60 month pain information as the outcome variable, T-1 analyzes the data a year before the pain appeared, T-2 analyzes the information two years before the pain appeared. GALGO an R package, was used to perform the analysis of 600 models of 5 features each, using a logistic regression as a classifier, with 3 k-fold cross validation, 66% of the data was used to train and the other 33% was used in a blind test. A forward selection models and robust gene backwards elimination were used to refine the final model. All statistical analysis was done using R software.
Results: All 6 models showed a pain predictive association. For quantitative data: T0 information, the final model was a three feature model with an AUC of 0.652, T-1 information the final model was a two feature model with an AUC of 0.617, T-2 information the final model was a four feature model with an AUC of 0.674. For semi-quantitative data: T0 information the final model was a four variable model with an AUC of 0.687, T-1 information the final model was a four feature model with an AUC of 0.679, T-2 information the final model was a two feature model with an AUC of 0.641.
Conclusions: The results suggest that some early radiological features can be associated with OA symptoms, it is possible to achieve future pain prediction with multivariate models based on X-ray features. The

		Results				
	Model	**Feature**	**OK**	**P-value**	**CI 95%**	
		JSW200 medial JSW al x=0.200 [mm]	6.194	0.059	1.078	53.227
	T0	JSW225 medial JSW al x=0.225 [mm]	0.040	0.010	0.002	0.366
		JSW275 medial JSW al s=0.275 [mm]	12.029	0.001	3.229	63.611
Quantitative	**T-1**	JSW300 medial JSW al x=0.300 [mm]	1.756	0.070	0.984	3.352
		LJSW875 lateral JSW al x=0.850 [mm]	2.031	0.035	1.061	4.030
		JSW175 medial JSW al x=0.175 [mm]	0.354	0.096	0.101	1.194
	T-2	JSW150 medial JSW al x=0.150 [mm]	2.170	0.213	0.642	7.587
		JSW250 medial JSW al x=0.250 [mm]	0.232	0.107	0.032	1.232
		JSW275 medial JSW al x=0.275 [mm]	12.672	0.003	2.645	84.299
		XRSCTM sclerosis (OARSI) tibia med comp.	0.201	0.073	0.024	0.957
	T0	XRJSM joint space narrowing (OARSI) med. comp.	0.655	0.281	0.298	1.405
		XRSCFM sclerosis (OARSI) femur med. comp.	6.818	0.053	1.162	64.729
Semi-quantitative		XROSEM osteophytes (OARSI) femur med. comp.	2.372	0.006	1.338	4.610
		XROSFM osteophytes (OARSI) femur med. comp.	2.726	0.002	1.522	5.369
	T-1	XRSCFM chondrocal cinosis (Grades 0-1) med. comp.	7.874	0.031	1.426	64.665
		XRJSM joint space narrowing (OARSI) med. comp.	0.584	0.183	0.259	1.276
		XRSCTM sclerosis (OAR SI) tibia med. comp.	0.169	0.183	0.023	0.805
	T-2	XROSEM osteophytes (OARSI) femur med. comp.	2.313	0.006	1.320	4.449
		XRKL Kellgren and Lawrence (grades 0-4)	0.771	0.242	0.494	1.189